Numerical study of optical radiation specularly reflected from an oriented plate

O.V. Shefer

Tomsk State University
Institute of Atmospheric Optics,
Siberian Branch of the Russian Academy of Sciences, Tomsk

Received February 15, 2001

Specular reflection of optical radiation from an oriented plate is studied numerically as applied to bistatic polarization laser sensing of water ice crystal clouds. The equations for polarization characteristics and the scattering cross section are examined numerically depending on the orientation and refractive index of the particulate matter for the cases of polarized and unpolarized incident radiation. The regular dependence of light scattering characteristics on the crystal orientation is illustrated. Based on the results obtained, it is shown that the interpretation methods can be constructed for determining parameters of the medium under study.

Introduction

Water ice crystal clouds are atmospheric formations with a complex structure. They comprise particles of various shapes and size,[1] which can take some preferred and/or random orientation in space. At present, much attention is given to the study of ice clouds all over the world. Of particular interest are optical phenomena in the atmosphere that are caused by interaction of optical radiation with water ice crystals.[2,3] Such phenomenon as corona consisting of color rings can be observed in the atmosphere because of light diffraction on small randomly oriented crystals.[4] Depending on the sun position, refraction of light in hexagonal crystals leads to formation of halo. Sun-pillars result from reflection of sunlight from oriented particles of an extended shape. In spite of the fact that the physical nature of these optical phenomena is known for a long time, certain peculiar features of each of them are still to be studied.

Research into interaction of optical radiation with water ice-crystals allows revealing variations in the characteristics of scattered radiation depending on variations of microphysical, optical, and orientation properties of the scatterers. In our earlier paper,[5] we presented an optical model of an oriented plate crystal for studying the spatial distribution of scattered radiation in the rear hemisphere, as well as its power and polarization parameters. Reference 6 presents numerically calculated results on scattering characteristics as functions of the particle size, orientation, refractive index, and scattering angles.

As known, crystal clouds consist largely of particles having some preferred orientation. The crystal clouds include ice plates that have most stable spatial position along with particles of other shapes. Furthermore, it is just plate crystals that provide for most intense reflection. In the case of specular reflection of radiation from crystals, it is possible to simplify to a maximum degree the scheme for interpretation of data of bistatic polarization sensing, because scattering in this case is independent of some angular characteristics.[5] It is clear that to reduce the experiment to the needed scheme corresponding to specular reflection, we should take into account the peculiarities of scattering for various positions of a source, receiver, and particle. The results of this research can be used to study sun-pillars formed at reflection of light from horizontally oriented plates.

This paper continues the research begun in Refs. 5 and 6; it presents the results of numerical study of specular reflection of electromagnetic field at different parameters of a particle.

Statement of the problem

Polarized radiation is incident onto a round plate with the radius a and the refractive index $\tilde{n} = n + i\chi$ and specularly reflected from it. The positions of the particle, receiver (the signal is received along the direction opposite to the specular reflection), and source are connected with the absolute coordinate system through the corresponding pair of angles (φ_i, θ_i) $(i = 1, 2, 3)$. The bistatic optical arrangement of the experiment has been described in Ref. 5. Equations for scattering cross section have been obtained within the framework of physical optics. These equations relate the main parameters of the reflected radiation with the microphysical, optical, and orientation properties of the particles under study. The considered model allows analysis of transformation of both polarized and unpolarized radiation.

For studying numerically characteristics of light scattering, we use Eq. (1), which determines the scattering cross sections σ_{π_i}, each of which is proportional to the corresponding parameter of the Stokes vector of the reflected radiation I_{π_i}

0235-6880/01/08 607-06 $02.00

$$\sigma_{\pi_i} = \omega I_{\pi_i}, \quad (i = 1, 2, 3, 4). \tag{1}$$

The coefficient of proportionality ω includes, as factors, all the needed parameters that enter into the lidar equation. The value of ω is obviously the same for all the four equations relating the Stokes vector parameters to the scattering cross section. Note that although the values of σ_{π_i} cannot be determined from the corresponding lidar equations without invoking *a priori* information, their ratios

$$P_i = \frac{I_{\pi_i}}{I_{\pi_1}} = \frac{\sigma_{\pi_i}}{\sigma_{\pi_1}}, \quad (i = 2, 3, 4) \tag{2}$$

can be directly measured in the experiment. For laser sensing of disperse media, the source transforming linearly polarized radiation or radiation with circular polarization is often used. Therefore, for analysis of polarization properties of scattered radiation, we consider two parameters, P_2 and P_4, respectively, for the cases of linear and circular polarization of the incident radiation.

For the scattering cross sections, the following equations are valid[5]:

$$\begin{aligned}
\sigma_{\pi_1} &= W\left\{M_{11} + \frac{I_2}{I_1} M_{12} + \frac{I_3}{I_1} M_{13} + \frac{I_4}{I_1} M_{14}\right\}, \\
\sigma_{\pi_2} &= W\left\{M_{21} + \frac{I_2}{I_1} M_{22} + \frac{I_3}{I_1} M_{23} + \frac{I_4}{I_1} M_{24}\right\}, \\
\sigma_{\pi_3} &= W\left\{M_{31} + \frac{I_2}{I_1} M_{32} + \frac{I_3}{I_1} M_{33} + \frac{I_4}{I_1} M_{34}\right\}, \\
\sigma_{\pi_4} &= W\left\{M_{41} + \frac{I_2}{I_1} M_{42} + \frac{I_3}{I_1} M_{43} + \frac{I_4}{I_1} M_{44}\right\}.
\end{aligned} \tag{3}$$

The factor W is determined by the wave number and the angular function being the Fraunhofer integral; I_i ($i = 1, 2, 3, 4$) are parameters of the Stokes vector of the incident radiation; M_{ij} are elements of the Mueller matrix ($i = 1, 2, 3, 4$; $j = 1, 2, 3, 4$).

One of the informative parameters characterizing nonsphericity of a scatterer is the depolarization ratio[7]:

$$D = \frac{M_{11} - M_{22}}{M_{11} + M_{22}}. \tag{4}$$

At interaction of the unpolarized radiation with a crystal, the radiation partially polarizes. Numerical calculations of the parameter determined by the following equation

$$St = (I_{\pi_2}^2 + I_{\pi_3}^2 + I_{\pi_4}^2)^{1/2} / I_{\pi_1}. \tag{5}$$

allow the degree of polarization as a function of different parameters of the particles to be studied.

Discussion of numerical results

Let us analyze the results calculated numerically on the characteristics of radiation (wavelength $\lambda = 10.6$ μm) specularly reflected from a plate (radius $a = 120$ μm) at different directions of sensing. Note that variations of the azimuth angle φ_1 determine orientation of the polarization plane. Variation of the angle θ_1 at fixed azimuth angles φ_i ($i = 1, 2, 3$), as well as at the fixed receiver's viewing direction θ_2 (or particle position θ_3) corresponds to variation of the angle β (β is the angle between the sensing direction and the normal to the plate base). The curves representing dependences of the scattering characteristics on the azimuth angle φ_1 varying from 0 to 360° at specular reflection have mirror symmetry about $\varphi_1 = 180°$ for the cases of polarized and unpolarized incident radiation.

Figure 1 shows numerically calculated scattering characteristics as functions of the azimuth angle φ_1 at three different positions of the particle with respect to the direction of radiation incidence.

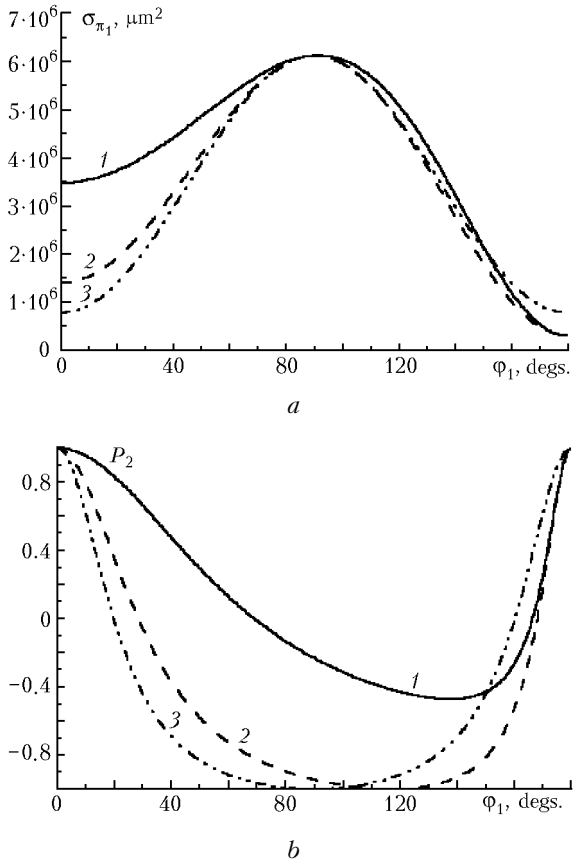

Fig. 1. Dependence of the scattering cross section $\sigma_{\pi_1}(\varphi_1)$ (*a*) and the polarization characteristic $P_2(\varphi_1)$ (*b*) at a linear polarization of incident radiation ($I_2/I_1 = 1$, $I_4 = I_3 = 0$) at $a = 125$ μm, $\lambda = 10.6$ μm, $\tilde{n} = 1.31 + i \cdot 10^{-4}$, $\varphi_2 = 0°$, $\theta_2 = 100°$, $\theta_1 = -40°$ (*1*), $-10°$ (*2*), and $0°$ (*3*).

The values of the characteristics at the initial point $\varphi_1 = 0°$ for the angles $\theta_1 = -40°$ (*1*), $\theta_1 = -10°$ (*2*), and $\theta_1 = 0°$ (*3*) are uniquely connected with the values of the angles β equal, respectively, to 60, 45, and 40°. As φ_1 increases from 0 to 180°, the angle β increases by several degrees.

As the angle φ_1 varies, we observe variations (see Fig. 1*a*) in the amplitude of the reflected signal. The rate of change of the scattering cross section at smaller β is higher (curve *3*) than at larger β (curve *1*). All the three curves have the same maximum for σ_{π_1} at $\varphi_1 = 90°$ (Fig. 1*a*) and minima of σ_{π_1} at $\varphi_1 = 0$ and 180°.

Figure 1*b* shows the dependences of the polarization characteristic $P_2(\varphi_1)$ in the case of linear polarization of the incident radiation. The position of minimum in each curve depends on the angle β. It is seen from Fig. 1*b* that the larger is the angle β, the higher is the point of minimum of the dependence $P_2(\varphi_1)$.

Figure 2*a* shows the degree of polarization *St* calculated by Eq. (5) at different positions of the particle for an unpolarized incident radiation. The curves illustrating the degree of polarization as a function of the azimuth angle φ_1 have steeper slopes at larger β.

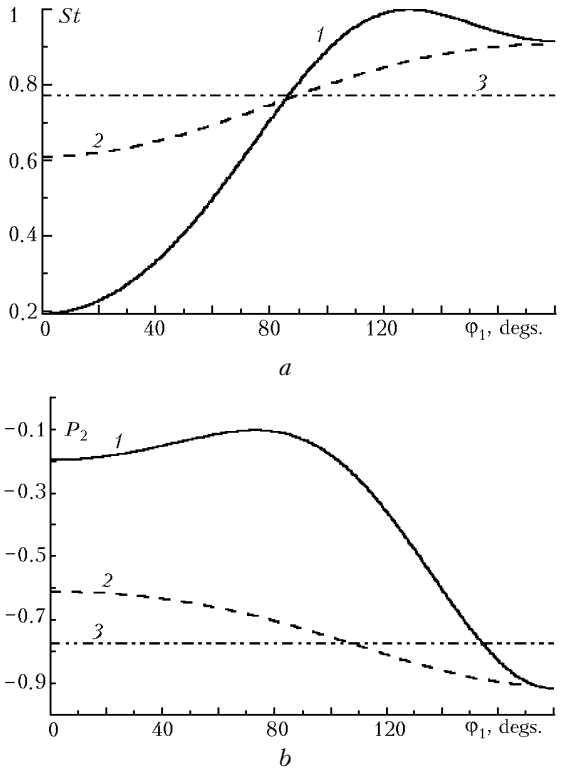

Fig. 2. Dependence of the degree of polarization $St(\varphi_1)$ (*a*) and the polarization characteristic $P_2(\varphi_1)$ (*b*) for an unpolarized incident radiation ($I_1 = 1$, $I_2 = I_4 = I_3 = 0$) at $a = 125$ μm, $\lambda = 10.6$ μm, $\tilde{n} = 1.31 + i \cdot 10^{-4}$, $\varphi_2 = 0°$, $\theta_2 = 100°$; $\theta_1 = -40°$ (*1*), $-10°$ (*2*), 0° (*3*).

It is seen from Fig. 2*b* that the unpolarized radiation after reflecting from a plate becomes almost completely linearly polarized as φ_1 varies from 120 to 180°. The character of variation of the polarization characteristic $P_2(\varphi_1)$ is more pronounced at larger β (curve *1* in Fig. 2*b*).

Under field conditions, the refractive index of cloud crystals may differ from the refractive index of pure water ice. In this connection, let us study numerically how the characteristics of reflected radiation depend on the optical properties of the plate. Figure 3*a* shows the dependence of the scattering cross section $\sigma_{\pi_1}(\varphi_1)$ on φ_1 for different refractive indices. The intensity of the reflected signal varies within one order of magnitude as the refractive index changes by 0.1, and the largest variations are observed at the points of maxima.

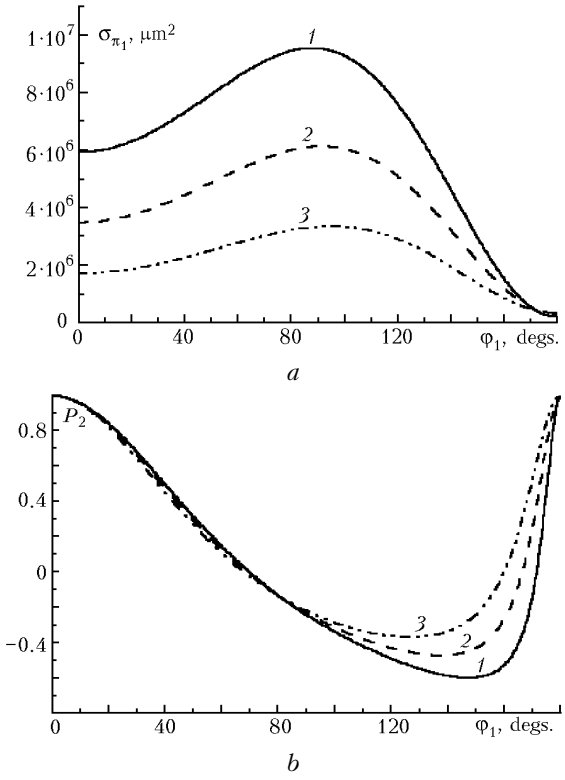

Fig. 3. Dependence of the scattering cross section $\sigma_{\pi_1}(\varphi_1)$ (*a*) and the polarization characteristic $P_2(\varphi_1)$ (*b*) at linear polarization of the incident radiation ($I_2/I_1 = 1$, $I_4 = I_3 = 0$) and $a = 125$ μm, $\lambda = 10.6$ μm, $\tilde{n} = n + i \cdot 10^{-4}$, $\varphi_2 = 0°$, $\theta_2 = 100°$, $\theta_1 = -40°$, $n = 1.42$ (*1*), 1.31 (*2*), 1.21 (*3*).

Figures 3*b* and 4*a* illustrate the variation of the scattering cross section ratios $P_2 = \sigma_{\pi_2}/\sigma_{\pi_1}$ and $P_4 = \sigma_{\pi_4}/\sigma_{\pi_1}$, respectively, for the linearly and circularly polarized incident radiation as functions of the azimuth angle φ_1 for different refractive indices of the plate.

The ratio P_2 equals 1, when the vector $\mathbf{E}_1$ of the linearly polarized incident wave (in this case $\mathbf{E}_2 = 0$) lies in the plane of incidence ($\varphi_1 = 0°$ or $\varphi_1 = 180°$). Every curve $P_2(\varphi_1)$ at the segment from 0 to 180° is asymmetric. One or another position of the point of minimum of the curve $P_2(\varphi_1)$ corresponds to a certain orientation of the plane of incidence of the electromagnetic wave and a certain value of the refractive index of the particle. The polarization characteristic $P_4(\varphi_1)$ for the case of circular

polarization of the incident radiation (Fig. 4*a*) has the highest rate of change as φ_1 varies from 80° to 180°. The values of P_4 for different refractive indices differ most widely at φ_1 close to 180°.

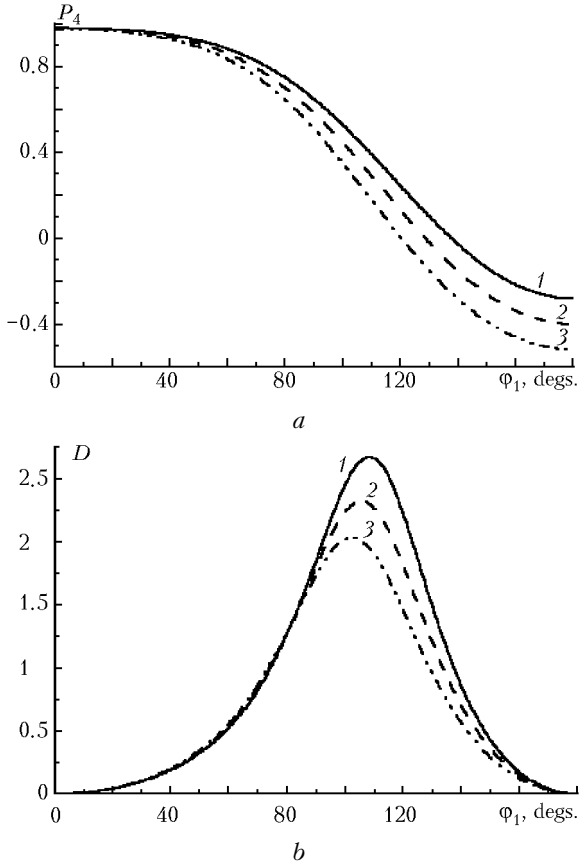

Fig. 4. Dependence of the polarization characteristic $P_4(\varphi_1)$ (*a*) and the depolarization ratio $D(\varphi_1)$ (*b*) at circular polarization of the incident radiation ($I_4/I_1 = 1$, $I_2 = I_3 = 0$) and $a = 125$ μm, $\lambda = 10.6$ μm, $\tilde{n} = n + i \cdot 10^{-4}$, $\varphi_2 = 0°$, $\theta_2 = 100°$, $\theta_1 = -40°$, $n = 1.42$ (*1*), 1.31 (*2*), 1.21 (*3*).

Figure 4*b* illustrates the dependence of the depolarization ratio D on φ_1 at different values of the refractive index (see Eq. (4)). The position of the only maximum in $D(\varphi_1)$ is uniquely connected with the variation of n. Note that the character of variation of the depolarization ratio $D(\varphi_1)$ is independent of the state of polarization of the incident radiation.

Figure 5 shows the dependences of the polarization characteristics for the case of an unpolarized radiation incident at an angle equal roughly to 60° for different values of the refractive index.

Note that the dependences $St(\varphi_1)$ (Fig. 5*a*) and $P_2(\varphi_1)$ (Fig. 5*b*) (curves *2*) were already shown in Figs. 2*a* and *b* (curves *1*), when we studied these characteristics $St(\varphi_1)$ and $P_2(\varphi_1)$ at different positions of the plate. It is seen from Fig. 5 that the values of St and P_2 for different refractive indices differ most widely at $\varphi_1 = 180°$. Note that variations of the degree of polarization St or the polarization characteristic P_2 are uniquely related to variations of the angle β of plate orientation with respect to the direction of radiation incidence and the refractive index. This, in its turn, suggests that the refractive index and the position of the crystal can be unambiguously determined from the data of passive sensing.

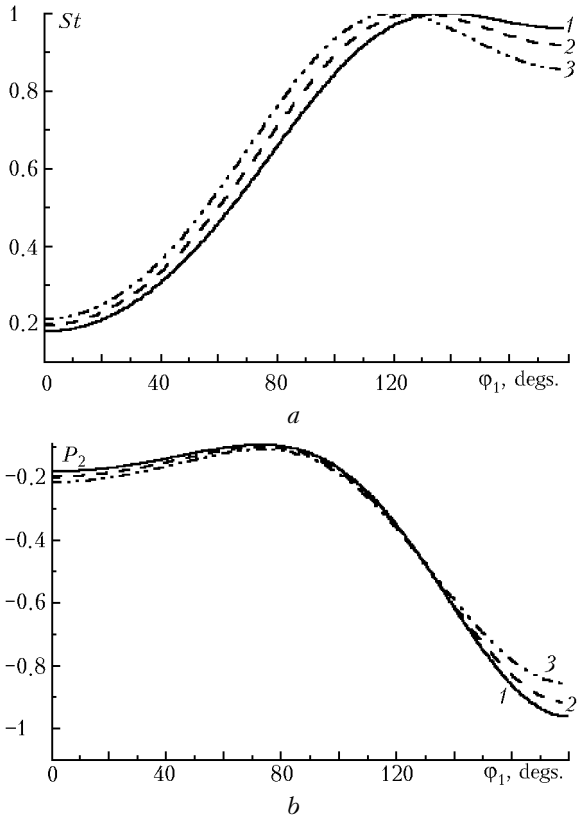

Fig. 5. Dependence of the degree of polarization $St(\varphi_1)$ (*a*) and the polarization characteristic $P_2(\varphi_1)$ (*b*) for an unpolarized incident radiation at $a = 125$ μm, $\lambda = 10.6$ μm, $\tilde{n} = n + i \cdot 10^{-4}$, $\varphi_2 = 0°$, $\theta_2 = 100°$, $\theta_1 = -40°$, $n = 1.42$ (*1*), 1.31 (*2*), 1.21 (*3*).

It should be noted that $\theta_1 = \beta$ is true for the dependences shown in Figs. 6–8. Figure 6 shows the function $\sigma_{\pi_1}(\theta_1)$ of the scattering cross section at different refractive indices of the particle, whose values are independent of the state of polarization of the incident radiation.

It is seen from the figure that the higher the refractive index, the higher the amplitude of the reflected signal. The differences in the absolute values of $\sigma_{\pi_1}(\theta_1)$ for different n are more pronounced at β ranging from 0 to 45°. It is the well known that the reflectivity of a water ice plate for β from 0 to 60° equals roughly 0.1, and for β from 60 to 90° it sharply increases up to 1. However, it is seen from Fig. 6 that the scattering cross section is higher for smaller β. This can be explained as follows. At numerical calculation of the scattering cross section, we should integrate over the area of the geometrical cross section of a particle in the considered direction of specular reflection, and the

larger the angle β, the smaller the projection area. Therefore, the calculated value of the scattering cross section σ_{π_1}, as an integral of the scattering characteristic over a larger area, exceeds the value of σ_{π_1} corresponding to the smaller cross section of the reflected beam. Note that the calculated characteristics shown in Fig. 6 correspond to $\varphi_1 = 0°$. In this case, the depolarization ratio D and the polarization characteristic P_2 bear no information.

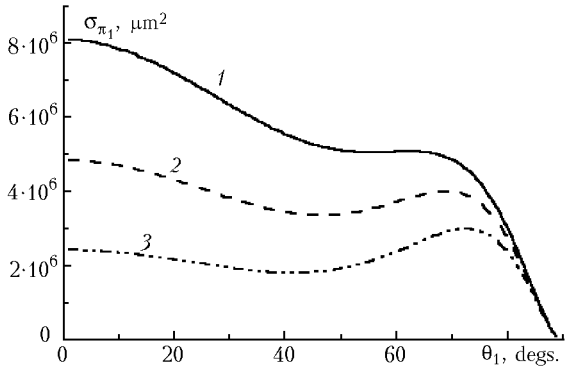

Fig. 6. Dependence of the scattering cross section $\sigma_{\pi_1}(\theta_1)$ for arbitrary state of polarization of the incident radiation at $a = 125$ μm, $\lambda = 10.6$ μm, $\tilde{n} = n + i \cdot 10^{-4}$, $\varphi_1 = 0°$, $\varphi_2 = 0°$, $\varphi_3 = 0°$, $\theta_2 = 180° - \theta_1$ ($\theta_1 = \beta$), $\theta_3 = 0°$, $n = 1.42$ (*1*), 1.31 (*2*), and 1.21 (*3*).

Figure 7 illustrates the dependence of the cross section ratio $P_4(\theta_1)$ at circular polarization of the incident radiation for different values of the refractive index n. The largest difference between the values of P_4 is observed for the angle β ranging from 40 to 70°.

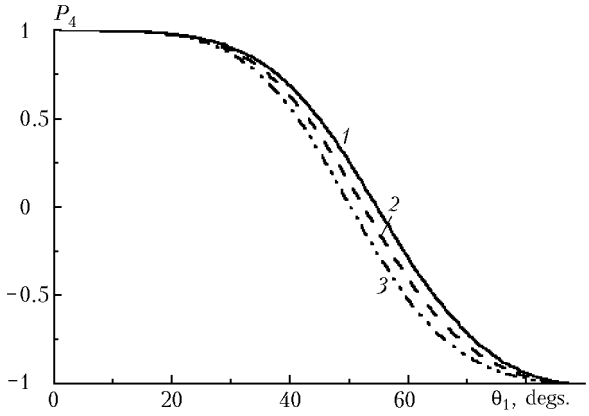

Fig. 7. Dependence of the scattering cross section ratio $P_4(\theta_1)$ at circular polarization of the incident radiation ($I_4/I_1 = 1$, $I_2 = I_3 = 0$) at $a = 125$ μm, $\lambda = 10.6$ μm, $\tilde{n} = n + i \cdot 10^{-4}$, $\varphi_1 = 0°$, $\varphi_2 = 0°$, $\varphi_3 = 0°$, $\theta_2 = 180° - \theta_1$ ($\theta_1 = \beta$), $\theta_3 = 0°$, $n = 1.42$ (*1*), 1.31 (*2*), and 1.21 (*3*).

The polarization characteristic remains practically unchanged $P_4 = 1$ at β ranging from 0 to 20° and P_4 equals roughly −1 at β ranging from 80 to 90°.

Figure 8 shows the dependences of the degree of polarization St and the polarization characteristic P_2 at different values of the refractive index of the plate versus the plate orientation with respect to the direction of incidence of the unpolarized radiation.

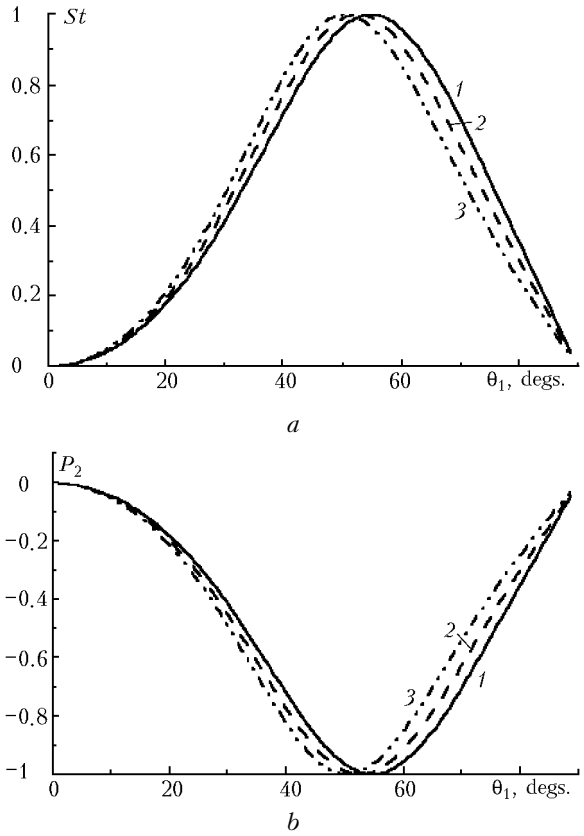

Fig. 8. Dependence of the degree of polarization $St(\theta_1)$ (*a*) and the polarization characteristic $P_2(\theta_1)$ (*b*) for the unpolarized incident radiation at $a = 125$ μm, $\lambda = 10.6$ μm, $\tilde{n} = n + i \cdot 10^{-4}$, $\varphi_1 = 0°$, $\varphi_2 = 0°$, $\varphi_3 = 0°$, $\theta_2 = 180° - \theta_1$ ($\theta_1 = \beta$), $\theta_3 = 0°$, $n = 1.42$ (*1*), 1.31 (*2*), and 1.21 (*3*).

The maximum of the degree of polarization, which falls on β from 50 to 60°, shifts to the right as the refractive index increases. The maximum in the St curve corresponds to the case that the incident unpolarized radiation becomes almost completely polarized after reflection from the plate. The polarization characteristic P_2 has a minimum at the point β corresponding to the highest degree of polarization, and the position of this minimum shifts at variation of n.

The dependence of the cross section of scattering by a plate was illustrated in Ref. 6 for the case different from the specular reflection. It was noted there that the increase in the scattering cross section is proportional to the increase in the plate size. Besides, the polarization characteristics such, for example, as the depolarization ratio and the scattering cross section ratio are independent of the particle size. Such a character of the dependence on the plate size for the cross section σ_{π_1} and the polarization characteristics is

observed for the case of specular reflection. The scattering cross section σ_{π_1} depends nonlinearly on the wavelength. The higher amplitude of the reflected signal corresponds to shorter wavelengths, all other input parameters being fixed. Integral characteristics, for example, the scattering coefficient, are of great interest for studying how scattering characteristics depend on the particle size and the wavelength, and numerical study of the scattering coefficient is the subject of our further research.

Conclusion

From analysis of theoretical results on the light scattering characteristics for optical radiation specularly reflected from an oriented plate, we have revealed regular dependences of the scattering cross section and polarization characteristics, such as the depolarization ratio and the scattering cross section ratio on the refractive index and orientation of a particle with respect to the source of radiation.

The results obtained from numerical simulation of interaction of a polarized radiation with a particle can be used for solution of direct and inverse problems as applied to bistatic polarization laser sensing in order to determine microphysical and optical properties, as well as orientation of the plates being a part of an ice crystal cloud.

Studies of the characteristics of an unpolarized radiation specularly reflected from an oriented plate, in particular, estimation of the amplitude of the reflected radiation and its degree of polarization give some knowledge on sun-pillars observed in the atmosphere to be taken into account when studying radiative transfer in the atmosphere. A detailed study of the scattering characteristics for an individual particle considered in this paper assumes further research into the corresponding integral parameters describing scattering by a polydisperse ensemble.

Acknowledgments

This work was partially supported by the Russian Foundation for Basic Research (Grant No. 01–05–65209).

References

1. O.A. Volkovitskii, L.N. Pavlova, and A.G. Petrushin, *Optical Properties of Ice Crystal Clouds* (Gidrometeoizdat, Leningrad, 1984), 200 pp.
2. A. Mallman, J.L. Hock, R.G. Greenler, Appl. Opt. **37**, 1441–1449 (1998).
3. K. Sassen, Appl. Opt. **37**, 1420–1426 (1998).
4. K. Sassen, J. Optics & Photonics News, No. 3, 39–42 (1999).
5. O.V. Shefer, Atmos. Oceanic Opt. **12**, No. 7, 549–553 (1999).
6. O.V. Shefer, Atmos. Oceanic Opt. **12**, No. 12, 1029–1036 (1999).
7. K-N. Liou and H. Lahore, J. Appl. Meteorol. **13**, No. 2, 257–263 (1974).